



# Photochemical degradation of carbofuran and elucidation of removal mechanism

Li-An Lu<sup>a</sup>, Ying-Shih Ma<sup>b</sup>, Mathava Kumar<sup>a</sup>, Jih-Gaw Lin<sup>a,\*</sup>

<sup>a</sup> Institute of Environmental Engineering, National Chiao Tung University, 1001, University Road, Hsinchu, Taiwan, ROC

<sup>b</sup> Department of Environmental Engineering and Health, Yuanpei University, 306 Yuanpei St., Hsinchu, Taiwan, ROC

## ARTICLE INFO

### Article history:

Received 8 June 2010

Received in revised form 18 October 2010

Accepted 18 October 2010

### Keywords:

Carbofuran

Dissolved organic carbon

Intermediates

Photo-Fenton reaction

Pseudo-first order reaction model

## ABSTRACT

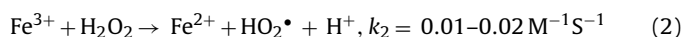
Carbofuran removal by the photo-Fenton reaction was investigated under various H<sub>2</sub>O<sub>2</sub> dosage rate (0–6 mg L<sup>-1</sup> min<sup>-1</sup>) and Fe<sup>3+</sup> dosage (5–50 mg L<sup>-1</sup>). The outcomes demonstrate that the photo-Fenton reaction was influenced by both the factors. An initial carbofuran concentration of 50 mg L<sup>-1</sup> was completely degraded within 30 min, and 93% dissolved organic carbon (DOC) removal was observed after 120 min of treatment at initial pH 3, H<sub>2</sub>O<sub>2</sub> dosage rate of 4 mg L<sup>-1</sup> min<sup>-1</sup> and Fe<sup>3+</sup> dosage of 35 and 50 mg L<sup>-1</sup>. However, no significant improvement in the carbofuran removal was observed when the H<sub>2</sub>O<sub>2</sub> dosage rate and Fe<sup>3+</sup> dosage were increased beyond 4 mg L<sup>-1</sup> min<sup>-1</sup> and 35 mg L<sup>-1</sup>, respectively. The carbofuran removal was fitted using the pseudo-first order reaction model and the highest apparent rate constant of 10.5 × 10<sup>-2</sup> min<sup>-1</sup> was obtained. Five major carbofuran intermediates were identified, which indicate that C–O bond of the carbamate group and 3-C position of the furan ring were oxidized as a result of the photo-Fenton reaction.

© 2010 Elsevier B.V. All rights reserved.

## 1. Introduction

Carbofuran (2,3-dihydro-2,2-dimethylbenzofuran-7-yl methyl-carbamate) is a broad spectrum carbamate pesticide and nematicide, which has been used against various foliar pests observed in fruit, vegetable and forest crops. It accounts about 12.4% of the total insecticides produced (14,493 tons) every year in Taiwan [1]. This carbamate pesticide is highly soluble in fresh water (700 mg L<sup>-1</sup>) [2]; therefore, it is susceptible to leaching and percolation through agricultural fields. Several researchers reported the presence of carbofuran in surface water and groundwater [3,4], and its half-life in water is ranging between 690 days at pH 5 and 7 days at pH 8 [4]. Hydrolysis and microbial degradation are the two most important mechanisms determining the stability of carbofuran in the environment. It is resistant to biological treatment methods; therefore, microbial degradation of this pesticide, i.e. biodegradation, requires longer time and specific microorganisms. Several treatment techniques including both physicochemical and biological methods could be applied for treating pesticide contaminated water. However, few techniques are sufficiently broad-based and convenient for real-time applications [5]. Since carbofuran exhibits a special biorefractory character and requires longer biodegradation time, its complete degradation in a shorter time could only be achieved by utilizing strong oxidizing agents.

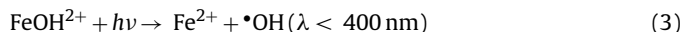
Advanced oxidation processes (AOPs) have been extensively investigated for water and wastewater treatments. These processes could be applied as the sole treatment process or as a pretreatment for improving the biodegradability of pesticide containing wastewater prior to the biological treatments [6–8]. Several studies have proven that AOPs are promising and also attractive alternatives in the treatment of organic pollutants that are either toxic or refractory to the biological treatments [9–12]. AOPs mainly rely on the generation of highly oxidative free radicals, in most cases the hydroxyl radical ( $\bullet\text{OH}$ ) with an  $E^0$  of 2.8 V/SHE [13]. A variety of effective treatment techniques such as ultrasonic irradiation, direct photolysis, ultra-violet (UV) irradiation in the presence of ozone or Fenton reagent, electro-Fenton, anodic Fenton treatment (AFT), TiO<sub>2</sub> as a photocatalyst and ultrasound penetration have been successfully applied for carbofuran degradation in contaminated water [4,14–20]. One of the AOPs, i.e. Fenton treatment, has been receiving more attention because of its broad-spectrum of target compounds, strong oxidation ability and fast reaction rate. In addition, it is simple, non-expensive and can be operated under the conditions of low temperature and atmospheric pressure [21]. The mechanism of the Fenton reaction with H<sub>2</sub>O<sub>2</sub> and Fe<sup>2+</sup> is shown in Eq. (1) and the generation of less powerful hydroperoxyl radical (HO<sub>2</sub> $\bullet$ ,  $E^0$  1.42 V/SHE) is shown in Eq. (2) [22–25].



The reaction rate of the Fenton reaction ( $k_1$ ) is much faster than the Fe<sup>2+</sup> regeneration rate ( $k_2$ ), therefore the addition of Fe<sup>2+</sup> and H<sub>2</sub>O<sub>2</sub>

\* Corresponding author. Tel.: +886 3 5722681; fax: +886 3 5725958.  
E-mail address: [jglin@mail.nctu.edu.tw](mailto:jglin@mail.nctu.edu.tw) (J.-G. Lin).

is required to keep the reaction proceeding. The major drawbacks of Fenton treatment are (1) the continuous addition of  $\text{Fe}^{2+}$  and  $\text{H}_2\text{O}_2$  for further oxidation of organic compound owing to the very slow regeneration of  $\text{Fe}^{2+}$  in Eq. (2), and (2) the production of large volume of ferric hydroxide sludge [26–28]. The photo-Fenton reaction, a combination of  $\text{H}_2\text{O}_2$  and UV irradiation less than 400 nm with  $\text{Fe}^{3+}$  or  $\text{Fe}^{2+}$ , is a promising treatment, which can produce relatively more  $\cdot\text{OH}$  compared to the Fenton treatment. This is mainly by the photoreduction of  $\text{Fe}(\text{OH})_2^{2+}$  (formed in the Fenton reaction at pH 2–3) to  $\text{Fe}^{2+}$  as shown in Eq. (3) [24]. Subsequently, the regenerated  $\text{Fe}^{2+}$  could undergo further reaction with more  $\text{H}_2\text{O}_2$  molecules, produce new  $\cdot\text{OH}$  and form a reaction cycle [23,29]. It has two advantages, i.e. (1) facilitate the Fenton treatment without continuous addition of external  $\text{Fe}^{2+}$ , and (2) reduce the ferric hydroxide sludge formation [23,30].



In the past, the photo-Fenton treatment has shown very high efficiency in the mineralization of biorefractory pesticides and other organic pollutants [9,21,30–33]. However, it is essential to estimate the best reaction condition or the complete mineralization of target compound, i.e. the initial pH and the dosages of  $\text{H}_2\text{O}_2$  and  $\text{Fe}^{3+}$  [21,30]. In this study, degradation/mineralization of carbofuran under the photo-Fenton reaction was investigated. The effects of dosage of  $\text{Fe}^{3+}$  and the dosage rate of  $\text{H}_2\text{O}_2$  on the performance of the photo-Fenton reaction were evaluated with continuous addition of  $\text{H}_2\text{O}_2$ . Moreover, the intermediates of carbofuran produced during the photo-Fenton treatment were identified by GC/MS. Based on the intermediates detected, the possible carbofuran degradation pathway was proposed.

## 2. Materials and methods

### 2.1. Chemical reagents

Carbofuran was obtained from Shida Chemical Industries (Taoyuan, Taiwan) and was used as received (HPLC grade, 98% purity). Titanium sulfate ( $\text{TiSO}_4$ , 5% w/w) was purchased from Nacalai Tesque (Japan) and hydrogen peroxide ( $\text{H}_2\text{O}_2$ , 33% w/w) was supplied by Panreac Chemicals (Spain). Exactly  $1000 \text{ mg L}^{-1}$   $\text{Fe}^{3+}$  stock solution was prepared by dissolving ferric sulfate ( $\text{Fe}_2(\text{SO}_4)_3$ ), Yakuri Pure Chemicals, Japan) and used for the experiments. The HPLC grade methanol was used in carbofuran analysis. All other chemicals were of reagent grade and the solutions were prepared using double distilled water.

### 2.2. Experimental apparatus

Fig. 1 represents the schematic diagram of the experimental setup. A 1.6L double-walled reactor was used in all the experiments. Several ports were provided in the reactor for feeding the reactants and sampling the solution. Moreover, pH and temperature probes were permanently fixed in the reactor. A Teflon-coated stirrer was installed in the reactor to mix the solution at 175 rpm. During the experiment,  $\text{H}_2\text{O}_2$  was added continuously into the reactor at a flow rate of  $1 \text{ mL min}^{-1}$  with a syringe pump. Two 8-W monochromatic UV lamps of 312 nm (with emission range between 280 nm and 360 nm) were placed axially in the reactor and kept in place with a quartz sleeve; the UV intensity of one 8-W UV lamp is  $60 \mu\text{W cm}^{-2}$ . The reaction temperature was maintained at  $25 \pm 1 \text{ }^\circ\text{C}$  by using a water bath.

### 2.3. Experimental procedures

Stock carbofuran solution was prepared by dissolving 200 mg of carbofuran in 1 L of double distilled water. Exactly 1 L of diluted

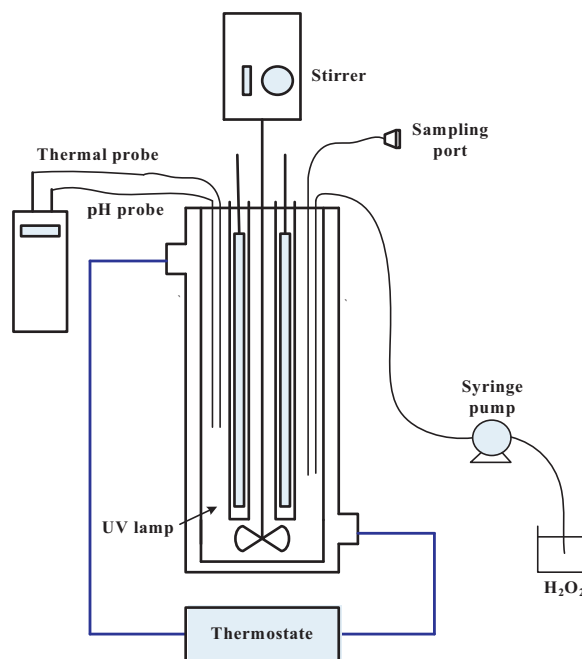


Fig. 1. Schematic diagram of the experimental setup.

carbofuran solution corresponding to an initial concentration of  $50 \text{ mg L}^{-1}$  was added into reactor. The initial pH was adjusted to 3 using 0.1N  $\text{H}_2\text{SO}_4$  [21,34–36]. Subsequently, a designed quantity of  $\text{Fe}^{3+}$  was added into the reactor and the contents were mixed thoroughly. The UV lamp was then turned on to mark the start point of the experiment and continued with the simultaneous addition of  $\text{H}_2\text{O}_2$  at a constant flow rate. At regular intervals, 8 mL of sample was withdrawn from the reactor and filtered through a  $0.45 \mu\text{m}$  membrane filter paper. Finally, the samples were analyzed for residual carbofuran, DOC,  $\text{H}_2\text{O}_2$  and carbofuran intermediates.

### 2.4. Analytical measurements

Carbofuran concentration in the samples was analyzed by the high performance liquid chromatography (HPLC) (Hitachi Co., Japan) equipped with a Hitachi L-2420 UV detector and a RP-18 GP 250 separation column ( $250 \text{ mm} \times 4.6 \text{ mm i.d.}$ , Kanto Chemicals, Japan). Exactly  $20 \mu\text{L}$  of sample was injected manually and analyzed at 280 nm. The mobile phase was composed of methanol and water (50:50, v/v), and was pumped at a flow rate of  $1 \text{ mL min}^{-1}$ . Under these separation conditions, the retention time of carbofuran was observed around 12 min. For determining the residual  $\text{H}_2\text{O}_2$  concentration, the samples were mixed with 5% titanium sulfate solution (the volume ratio of  $\text{H}_2\text{O}_2$  sample to titanium sulfate solution is 10:1, v/v) and analyzed in a spectrophotometer (Hitachi U-3010, Japan) at 412 nm. The residual  $\text{H}_2\text{O}_2$  was measured for two purposes: (1) to make sure that the  $\text{H}_2\text{O}_2$  supplied in the system is sufficient, and (2) to compare the residual  $\text{H}_2\text{O}_2$  with the variation of carbofuran concentration and DOC removal. Carbofuran mineralization was estimated from DOC concentrations. A TOC analyzer (O.I. Analytical Model 1030) was adopted for measuring the DOC of the samples. Throughout the study, the reaction pH and temperature were continuously monitored by a pH probe and thermometer (Suntex TS-2, Taiwan), respectively.

### 2.5. Identification of major intermediates

The major carbofuran intermediates formed during the photo-Fenton reaction were identified using the GC/MS technique. A

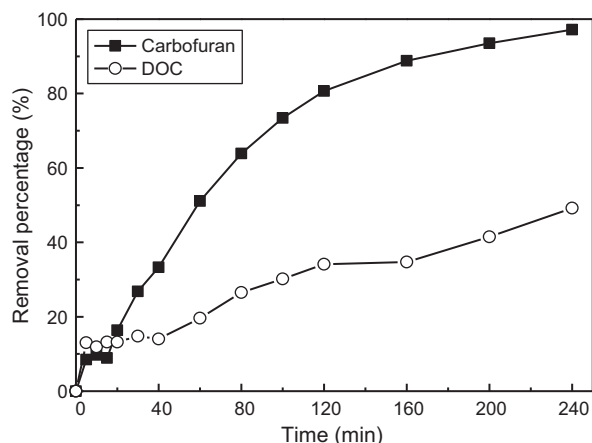


Fig. 2. The profile of carbofuran and DOC removal percentages with time ( $\text{Fe}^{3+}$  dosage at  $5 \text{ mg L}^{-1}$ ,  $\text{H}_2\text{O}_2$  dosage rate at  $0.1 \text{ mg L}^{-1} \text{ min}^{-1}$  and pH 3).

mixture of sample and dichloromethane (5:1, v/v) was shaken vigorously in a rotary shaker at 150 rpm for 30 min, and subsequently, analyzed in a Shimadzu GC/MS-QP2010 equipped with a HP-5 capillary column (30 m  $\times$  0.25 mm i.d., thickness of 0.25  $\mu\text{m}$ ). Helium was used as the carrier gas at a flow rate of  $1.5 \text{ mL min}^{-1}$ . The GC oven temperature was programmed as follows: initially held at  $80^\circ\text{C}$  for 2 min, increased to  $210^\circ\text{C}$  at a rate of  $10^\circ\text{C min}^{-1}$  and held for 3 min, then raised from  $210$  to  $310^\circ\text{C}$  at a rate of  $30^\circ\text{C min}^{-1}$  and finally held at  $310^\circ\text{C}$  for 2 min. The injector and detector temperatures were maintained at  $220$  and  $250^\circ\text{C}$ , respectively. The mass spectrometer was operated in the full-scan electron-impact (EI) mode at  $70 \text{ eV}$ .

### 2.6. Carbofuran removal kinetics

The pseudo-first order reaction model as shown in Eq. (4) was used to study the carbofuran removal kinetics.

$$\ln\left(\frac{C_0}{C_t}\right) = k_{app}t \quad (4)$$

where  $C_0$  and  $C_t$  are the concentrations of carbofuran ( $\text{mg L}^{-1}$ ) at reaction times zero and  $t$ .  $k_{app}$  is the apparent rate constant ( $\text{min}^{-1}$ ) and  $t$  is the reaction time (min). The rate constants are estimated based on the linear plot of  $\ln(C_0/C_t)$  versus  $t$ .

## 3. Results and discussion

### 3.1. Effect of irradiation time on carbofuran degradation

The UV irradiation time required for carbofuran degradation was evaluated under an initial carbofuran concentration of  $50 \text{ mg L}^{-1}$  and pH 3 with the  $\text{Fe}^{3+}$  dosage at  $5 \text{ mg L}^{-1}$  and  $\text{H}_2\text{O}_2$  dosage rate at  $0.1 \text{ mg L}^{-1} \text{ min}^{-1}$ . The profiles of carbofuran and DOC removal percentages are shown in Fig. 2. After 240 min, carbofuran and DOC

removals were reached around 97% and 42%, respectively. These results indicate that even with low dosage of  $\text{Fe}^{3+}$  and dosage rate of  $\text{H}_2\text{O}_2$ , it is possible to obtain higher carbofuran degradation as well as its mineralization. However, no significant increase in the carbofuran removal was observed between 120 and 240 min (less than 10%). The DOC removal profile indicates that carbofuran mineralization rate could be enhanced by increasing the UV irradiation time. However, considering the carbofuran removal, 120 min was adopted for the subsequent experiments.

### 3.2. Effect of $\text{H}_2\text{O}_2$ dosage rate on carbofuran degradation

In order to identify a better dosage of  $\text{H}_2\text{O}_2$  required for the photo-Fenton reaction, the experiments were repeated at pH 3, with a  $\text{Fe}^{3+}$  dosage of  $35 \text{ mg L}^{-1}$  and varying  $\text{H}_2\text{O}_2$  dosage rates ( $0\text{--}6 \text{ mg L}^{-1} \text{ min}^{-1}$ ). Carbofuran and DOC removals under various dosage rates of  $\text{H}_2\text{O}_2$  are shown in Table 1. Throughout the experiments, the solution pH remains relatively unchanged (2.8–3.4). It can be noticed in the experimental outcomes that the carbofuran degradation increases under the higher dosage rates of  $\text{H}_2\text{O}_2$ , which is mainly due to the generation of  $\cdot\text{OH}$  with extra  $\text{H}_2\text{O}_2$  addition. On the other hand, carbofuran removals have improved greatly, i.e. 32–73%, 39–90% and 47–100% within 15, 20 and 30 min reaction, respectively, when the  $\text{H}_2\text{O}_2$  dosage rate was increased from 0 to  $4 \text{ mg L}^{-1} \text{ min}^{-1}$  (Table 1). At the same condition, the DOC removal efficiency has increased from 13% to 93% after 120 min reaction. However, no improvement in the carbofuran/DOC removal was observed when the  $\text{H}_2\text{O}_2$  was overdosed, i.e. beyond  $4 \text{ mg L}^{-1} \text{ min}^{-1}$ . Several researchers have also reported the negative effect of  $\text{H}_2\text{O}_2$  dosage under  $\text{H}_2\text{O}_2$  overdosed photo-Fenton systems for the degradation of target compound [21,37]. Under this overdosed rate,  $\text{H}_2\text{O}_2$  could react with  $\cdot\text{OH}$ , and as a result, less powerful  $\text{HO}_2\cdot$  is formed as shown in Eq. (5). Moreover,  $\text{HO}_2\cdot$  could further react with  $\cdot\text{OH}$  and form water and oxygen as per Eq. (6) [21,38]. Therefore, the  $\text{H}_2\text{O}_2$  dosage rate beyond  $4 \text{ mg L}^{-1} \text{ min}^{-1}$  can reduce the oxidative capacity of the photo-Fenton reaction by decreasing the amount of  $\cdot\text{OH}$  and oxidant in the system [36].



The DOC profile has shown a sharp increase from 10 to 60% within 20–60 min, and then, followed a gradual increase after 60 min (60–93%) at higher  $\text{H}_2\text{O}_2$  dosage rate. This is in good agreement with the residual  $\text{H}_2\text{O}_2$  concentration as shown in Fig. 3. The residual  $\text{H}_2\text{O}_2$  concentration under  $\text{H}_2\text{O}_2$  dosage rates of 4 and  $5 \text{ mg L}^{-1} \text{ min}^{-1}$  decrease at reaction time 15–40 min, and then, increases gradually after 40 min (Fig. 3). The carbofuran removals were fitted using the pseudo-first order reaction model; the highest apparent rate constant of  $8.8 \times 10^{-2} \text{ min}^{-1}$  was observed at the  $\text{H}_2\text{O}_2$  dosage rate of  $4 \text{ mg L}^{-1} \text{ min}^{-1}$  (Table 1). This reveals that  $\text{H}_2\text{O}_2$  dosage rate at  $4 \text{ mg L}^{-1} \text{ min}^{-1}$  has accelerated the oxidation rate of carbofuran.

Table 1  
Effect of various  $\text{H}_2\text{O}_2$  dosage rates on carbofuran and DOC removals ( $\text{Fe}^{3+}$  dosage at  $35 \text{ mg L}^{-1}$  and pH 3).

$\text{H}_2\text{O}_2$ dosage rate ( $\text{mg L}^{-1} \text{ min}^{-1}$ )	Carbofuran removal (%)			DOC removal (%)		Pseudo-first order carbofuran removal kinetics	
	15 min	20 min	30 min	30 min	120 min	$k_{app}$ ( $\times 10^{-2} \text{ min}^{-1}$ )	$R^2$
0	32	39	47	9	13	1.4	0.87
0.5	40	48	68	11	49	4.5	0.98
1.25	66	78	92	23	76	7.7	0.98
4	73	90	100	31	93	8.8	0.94
5	73	87	100	26	92	8.6	0.95
6	45	62	86	12	79	5.6	0.91

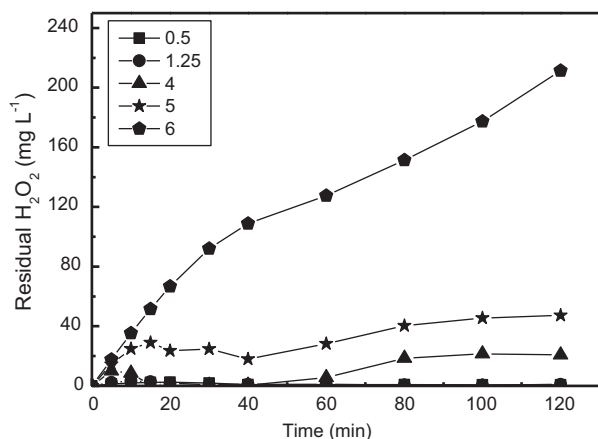


Fig. 3. Variation of residual H<sub>2</sub>O<sub>2</sub> as a function of time with different H<sub>2</sub>O<sub>2</sub> dosage rates (Fe<sup>3+</sup> dosage at 35 mg L<sup>-1</sup> and pH 3).

### 3.3. Effect of Fe<sup>3+</sup> on carbofuran degradation

The photo-Fenton experiments were repeated under different Fe<sup>3+</sup> dosages (5–50 mg L<sup>-1</sup>) and H<sub>2</sub>O<sub>2</sub> dosage rates (0.8 and 4 mg L<sup>-1</sup> min<sup>-1</sup>), and at fixed pH, i.e. pH 3. The experimental outcomes are shown in Table 2 and the H<sub>2</sub>O<sub>2</sub> consumption is shown in Fig. 4. Throughout the study not much variation in pH (2.9–3.3) was observed. Table 2 demonstrates that carbofuran and DOC removal efficiencies could be improved by increasing the Fe<sup>3+</sup> dosage. The increase in Fe<sup>3+</sup> dosage increases the production of more quantity of •OH through the Fenton reaction and facilitates the higher carbofuran and DOC removal efficiencies.

However, no significant improvement in carbofuran and DOC removals were observed when the Fe<sup>3+</sup> dosage was increased beyond 35 mg L<sup>-1</sup>. This is in good agreement with the results reported in the previous studies [21,23,39]. The main reason is for the limited degradation of carbofuran at H<sub>2</sub>O<sub>2</sub> dosage rate of 0.8 mg L<sup>-1</sup> min<sup>-1</sup> is due to the insufficient residual H<sub>2</sub>O<sub>2</sub> concentration in the system (Fig. 4). The higher removal at a H<sub>2</sub>O<sub>2</sub> dosage rate of 4 mg L<sup>-1</sup> min<sup>-1</sup> could be attributed to the increased residual H<sub>2</sub>O<sub>2</sub> concentration in the system; however, the increase in Fe<sup>3+</sup> dosage beyond 35 mg L<sup>-1</sup> at this condition has produced similar carbofuran removal owing to the photostationary equilibrium between Fe<sup>2+</sup> and Fe<sup>3+</sup> [4].

The carbofuran removals shown in Table 2 were fitted using the pseudo-first order reaction model. The apparent rate constants are

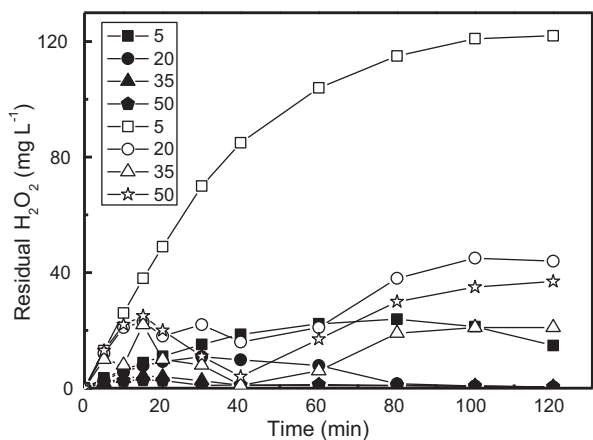


Fig. 4. Variation of residual H<sub>2</sub>O<sub>2</sub> as a function of time with different Fe<sup>3+</sup> dosages at pH 3 (solid points represent H<sub>2</sub>O<sub>2</sub> dosage rate at 0.8 mg L<sup>-1</sup> min<sup>-1</sup> and hollow points represent H<sub>2</sub>O<sub>2</sub> dosage rate at 4 mg L<sup>-1</sup> min<sup>-1</sup>).

shown in Table 2, which indicate that the increase in Fe<sup>3+</sup> dosages and the dosage rates of H<sub>2</sub>O<sub>2</sub> have the capability of increasing the carbofuran removal rate to a certain extent. The highest carbofuran removal rate constant of  $10.5 \times 10^{-2} \text{ min}^{-1}$  was observed at 50 mg L<sup>-1</sup> Fe<sup>3+</sup> dosage with 4 mg L<sup>-1</sup> min<sup>-1</sup> of H<sub>2</sub>O<sub>2</sub> dosage rate.

### 3.4. Chemical degradability of carbofuran

A summary of experiments and the main outcomes are given in Table 3. This could be useful to evaluate the efficiency of each process in carbofuran degradation/mineralization. It can be seen in Table 3 that no carbofuran volatilization was observed in 120 min reaction; therefore, the carbofuran removal in the present study was solely by the treatment technique adopted. The simple oxidation techniques, i.e. H<sub>2</sub>O<sub>2</sub>, Fe<sup>3+</sup>, UV irradiation and the combination of H<sub>2</sub>O<sub>2</sub> and Fe<sup>3+</sup>, have produced fewer carbofuran removal and insignificant DOC removal efficiencies. While H<sub>2</sub>O<sub>2</sub> and Fe<sup>3+</sup> were combined with UV irradiation, i.e. UV + H<sub>2</sub>O<sub>2</sub> and UV + Fe<sup>3+</sup>, the carbofuran removal was increased to 84% and 77%, respectively, after 120 min reaction. However, the DOC removal has reached only less than 17% in these combinations.

On the other hand, the photo-Fenton reaction has produced complete carbofuran removal (100%) in 30 min and up to 93% DOC removal in 120 min. These results indicate that the photo-Fenton treatment is highly effective for the rapid degradation and mineralization of carbofuran. Also, the photo-Fenton system was reported as the most efficient process for the degradation of several pollutants [21,31,33]. In this study, H<sub>2</sub>O<sub>2</sub> was supplied at a constant flow rate during the treatment, which could minimize the reagent cost. As a whole, the application of the photo-Fenton reaction with constant supply of H<sub>2</sub>O<sub>2</sub> can generate rapid removal of carbofuran from aqueous systems.

### 3.5. Degradation pathway

The experimental samples collected under the photo-Fenton conditions, i.e. Fe<sup>3+</sup> dosage at 35 mg L<sup>-1</sup>, H<sub>2</sub>O<sub>2</sub> dosage rate at 4 mg L<sup>-1</sup> min<sup>-1</sup> and at pH 3, were used for identifying the intermediates of carbofuran and the degradation pathway. Five major intermediates, i.e. 3-Hydroxy-2,2-dimethyl-2,3-dihydro-1-benzofuran-7-yl methylcarbamate, 2,2-Dimethyl-3-oxo-2,3-dihydro-1-benzofuran-7-yl methylcarbamate, 2,2-Dimethyl-2,3-dihydro-1-benzofuran-7-ol, 2,2-Dimethyl-2,3-dihydro-1-benzofuran-3,7-diol and 7-Hydroxy-2,2-dimethyl-1-benzofuran-3(2H)-one, were identified and their full scan mass spectra are shown in Fig. 5(b–f), respectively. Based on the spectral analysis of the intermediates, the possible carbofuran degradation pathway(s) are proposed in Fig. 6, and numbers 1–5 are assigned to five intermediates. The first step in the degradation of carbofuran is found to be the cleavage of C–O bond in carbamate group and the formation of intermediate 1 (*m/z* 164) [40]. This intermediate has also been detected in the photolysis, TiO<sub>2</sub> catalyzed photolysis and anodic Fenton treatment of carbofuran [16,40,41]. The carbamate group appeared to be the primary attack site by •OH in the photo-Fenton reaction. Alternatively, it is envisaged that hydroxylation of carbofuran and intermediate 1 also play an important role in the initial degradation owing to •OH attack at the 3-C position of furan ring. This leads to the formation of intermediates 2 (*m/z* 237) and 3 (*m/z* 180) [42]. The successive oxidation of these two compounds, i.e. *m/z* 237 and 180, at their 3-C position of the furan ring might have induced the formation of intermediates 4 (*m/z* 235) and 5 (*m/z* 178) [24].

In addition to the hydroxylation and further oxidation of 3-C position in the furan ring, the cleavage of carbamate group from intermediates 2 and 4 can also result in the formation

**Table 2**  
Effect of various Fe<sup>3+</sup> dosages on carbofuran and DOC removals at pH 3.

H <sub>2</sub> O <sub>2</sub> dosage rate (mg L <sup>-1</sup> min <sup>-1</sup> )	Fe <sup>3+</sup> dosage (mg L <sup>-1</sup> )	Carbofuran removal (%)			DOC removal (%)		Pseudo-first order carbofuran removal kinetics	
		15 min	20 min	30 min	30 min	120 min	<i>k</i> <sub>app</sub> (×10 <sup>-2</sup> min <sup>-1</sup> )	R <sup>2</sup>
0.8	5	6	17	40	0	46	2.6	0.95
	20	34	41	64	12	59	4.4	0.92
	35	54	68	81	16	62	6.5	0.98
	50	58	72	85	19	63	6.9	0.99
4	5	42	54	79	9	79	5.2	0.96
	20	71	85	100	32	91	8.3	0.96
	35	73	90	100	31	93	8.6	0.94
	50	80	97	100	34	93	10.5	0.94

**Table 3**  
Carbofuran and DOC removals under different experimental conditions.

Experiment	H <sub>2</sub> O <sub>2</sub> (mg L <sup>-1</sup> min <sup>-1</sup> )	Fe <sup>3+</sup> (mg L <sup>-1</sup> )	Carbofuran (mg L <sup>-1</sup> )	pH	Removals after 120 min	
					Carbofuran (%)	DOC (%)
Control	0	0	50	3	0	0
UV	0	0	50	3	7	0
H <sub>2</sub> O <sub>2</sub>	4	0	50	3	10	0
Fe <sup>3+</sup>	0	35	50	3	0	0
Fe <sup>3+</sup> + H <sub>2</sub> O <sub>2</sub>	4	35	50	3	18	5
UV + H <sub>2</sub> O <sub>2</sub>	4	0	50	3	84	17
UV + Fe <sup>3+</sup>	0	35	50	3	77	13
Photo-Fenton <sup>a</sup>	4	35	50	3	100	93

<sup>a</sup> UV + Fe<sup>3+</sup> + H<sub>2</sub>O<sub>2</sub>.

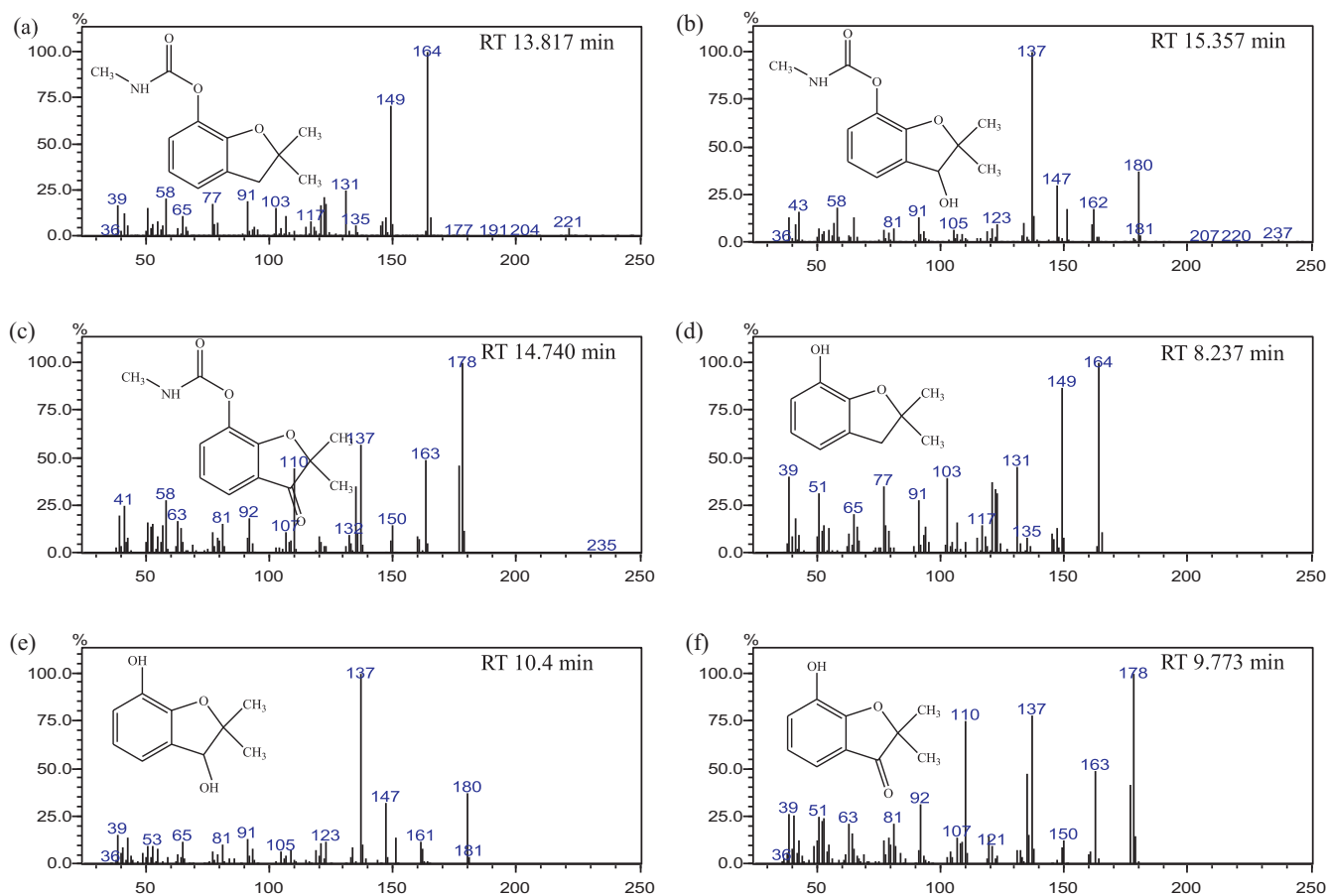


**Fig. 5.** GC-MS spectra of carbofuran and its degradation intermediates (RT means retention time).

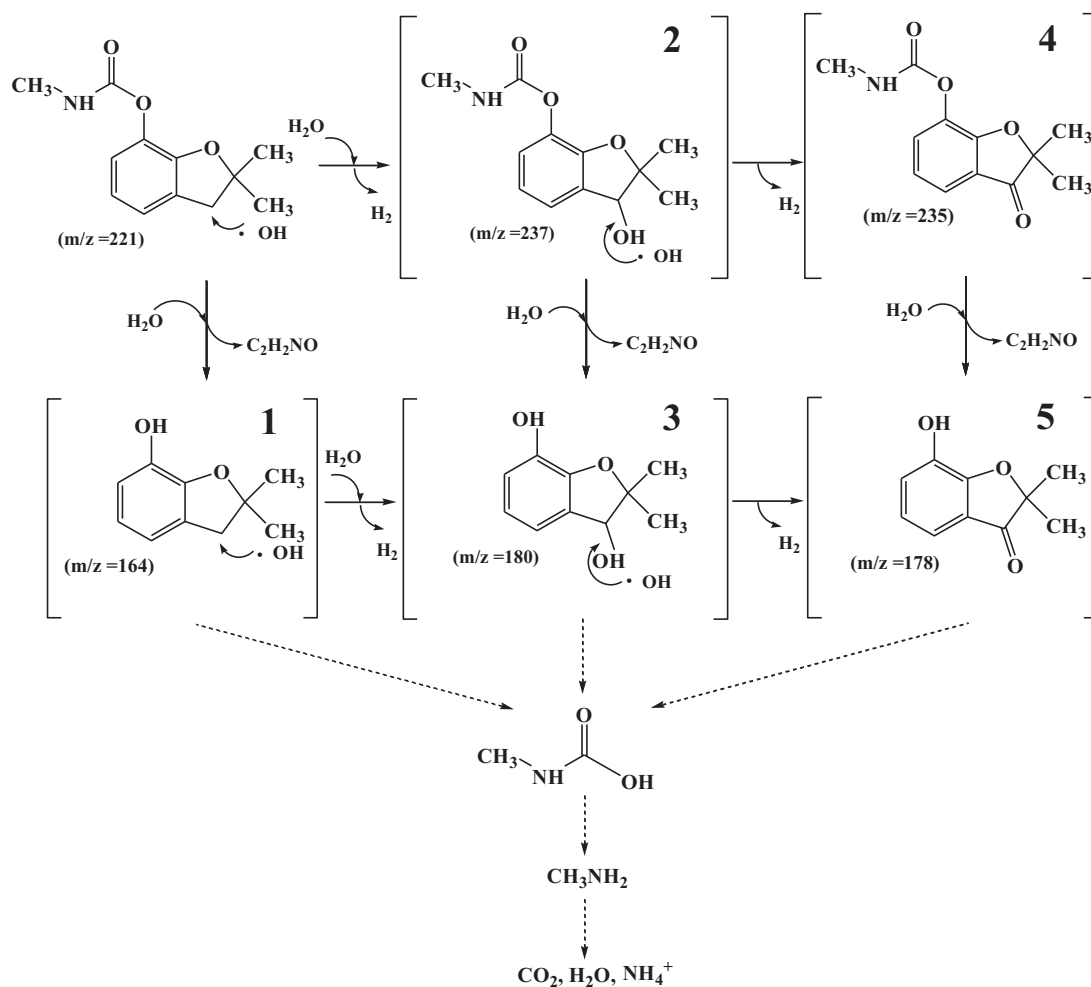


Fig. 6. Proposed degradation pathways of carbofuran by photo-Fenton process (dotted lines reflect the hypothesized carbofuran degradation pathway).

of intermediates 3 and 5. Moreover, the decrease of DOC up to 93% (Table 3) indicates that the furan ring or benzene ring is opened, and subsequently, mineralized to inorganic carbon dioxide and water via carbamic acid and methyl amine as reported in previous investigations [4,16]. In addition to these five compounds, there may be other intermediates of carbofuran, which are not detected at this moment owing to their lower concentrations.

#### 4. Conclusions

Carbofuran degradation was accelerated in the photo-Fenton system and the apparent degradation rate was influenced by many factors such as irradiation time, the dosage rate of  $\text{H}_2\text{O}_2$  and dosage of  $\text{Fe}^{3+}$  applied. The pseudo-first order reaction kinetics was used to model the carbofuran removal in the system. A highest carbofuran removal rate constant of  $10.5 \times 10^{-2} \text{ min}^{-1}$  was obtained under an initial pH of 3,  $\text{Fe}^{3+}$  dosage of  $50 \text{ mg L}^{-1}$  and  $\text{H}_2\text{O}_2$  dosage rate of  $4 \text{ mg L}^{-1} \text{ min}^{-1}$ . Under these conditions, an initial carbofuran concentration of  $50 \text{ mg L}^{-1}$  was completely degraded and 93% of DOC removal was achieved in 120 min reaction. Furthermore, five intermediate products of carbofuran were identified during the photo-Fenton reaction and the degradation pathway(s) were proposed. As a whole, the photo-Fenton treatment has greater potential for carbofuran removal in comparison with other AOPs.

#### Acknowledgements

The authors would like to thank the National Science Council, Taiwan, ROC for the financial support (98-2221-E-009-022-MY3). They also thank Professor C.S. Chiou, Department of Environmental Engineering, National Ilan University for the experimental assistance.

#### References

- [1] C. Yuan, Annual report of Taiwan's agriculture, Council of Agriculture (2008).
- [2] C.W. Worthing, The Pesticide Manual, 9th ed., British Crop Protection Council, London, 1991.
- [3] R. Jaramillo, W. Bowen, J. Stoorvogel, Carbofuran presence in soil leachate, groundwater, and surface water in the potato growing area in Carchi, Ecuador, CIP Program Report for 1999–2000 (2001) 355–360.
- [4] H. Katsumata, K. Matsuba, S. Kaneco, T. Suzuki, K. Ohta, Y. Yobiko, Degradation of carbofuran in aqueous solution by Fe (III) aquacomplexes as effective photocatalysts, J. Photochem. Photobiol. A 170 (3) (2005) 239–245.
- [5] P.L. Huston, J.J. Pignatello, Degradation of selected pesticide active ingredients and commercial formulations in water by the photo-assisted Fenton reaction, Water Res. 33 (5) (1999) 1238–1246.
- [6] S. Malato, J. Blanco, A. Vidal, D. Alarcon, M.I. Maldonado, J. Caceres, W. Gernjak, Applied studies in solar photocatalytic detoxification: an overview, Sol. Energy 75 (4) (2003) 329–336.
- [7] A.M. Amat, A. Arques, A. Garcia-Ripoll, L. Santos-Juanes, R. Vicente, I. Oller, M.I. Maldonado, S. Malato, A reliable monitoring of the biocompatibility of an effluent along an oxidative pre-treatment by sequential bioassays and chemical analyses, Water Res. 43 (3) (2009) 784–792.
- [8] C. Sirtori, A. Zapata, I. Oller, W. Gernjak, A. Aguera, S. Malato, Decontamination industrial pharmaceutical wastewater by combining solar photo-Fenton and biological treatment, Water Res. 43 (3) (2009) 661–668.

- [9] W.C. Paterlini, R.F.P. Nogueira, Multivariate analysis of photo-Fenton degradation of the herbicides tebuthiuron, diuron and 2,4-D, *Chemosphere* 58 (8) (2005) 1107–1116.
- [10] J.J. Pignatello, E. Oliveros, A. MacKay, Advanced oxidation processes for organic contaminant destruction based on the Fenton reaction and related chemistry, *Crit. Rev. Environ. Sci. Technol.* 36 (1) (2006) 1–84.
- [11] A. Arques, A.M. Amat, A. Garcia-Ripoll, R. Vicente, Detoxification and/or increase of the biodegradability of aqueous solutions of dimethoate by means of solar photocatalysis, *J. Hazard. Mater.* 146 (3) (2007) 447–452.
- [12] E.C. Catalkaya, F. Kargi, Effects of operating parameters on advanced oxidation of diuron by the Fenton's reagent: a statistical design approach, *Chemosphere* 69 (3) (2007) 485–492.
- [13] E. Brillas, I. Sirès, M.A. Oturan, Electro-Fenton process and related electrochemical technologies based on Fenton's reaction chemistry, *Chem. Rev.* 109 (12) (2009) 6570–6631.
- [14] I. Hua, U. Pfaller-Thompson, Ultrasonic irradiation of carbofuran: decomposition kinetics and reactor characterization, *Water Res.* 35 (6) (2001) 1445–1452.
- [15] F.J. Benitez, J.L. Acero, F.J. Real, Degradation of carbofuran by using ozone, UV radiation and advanced oxidation processes, *J. Hazard. Mater.* 89 (1) (2002) 51–65.
- [16] M. Mahalakshmi, B. Arabindoo, M. Palanichamy, V. Murugesan, Photocatalytic degradation of carbofuran using semiconductor oxides, *J. Hazard. Mater.* 143 (1–2) (2007) 240–245.
- [17] Y.S. Ma, M. Kumar, J.G. Lin, Degradation of carbofuran-contaminated water by the Fenton process, *J. Environ. Sci. Health. Part A Toxic/Hazard. Subst. Environ. Eng.* 44 (9) (2009) 914–920.
- [18] Y.S. Ma, C.F. Sung, Investigation of carbofuran decomposition by a combination of ultrasonic and Fenton process, *Sustain. Environ. Res.* 20 (2010) 213–219.
- [19] A.K. Abdessalem, N. Bellakhal, N. Oturan, M. Dachraoui, M.A. Oturan, Treatment of a mixture of three pesticides by photo- and electro-Fenton processes, *Desalination* 250 (1) (2010) 450–455.
- [20] Y.S. Ma, C.F. Sung, J.G. Lin, Degradation of carbofuran in aqueous solution by ultrasound and Fenton processes: effect of system parameters and kinetic study, *J. Hazard. Mater.* 178 (1–3) (2010) 320–325.
- [21] M. Tamimi, S. Qourzal, N. Barka, A. Assabane, Y. Ait-Ichou, Methomyl degradation in aqueous solutions by Fenton's reagent and the photo-Fenton system, *Sep. Purif. Technol.* 61 (1) (2008) 103–108.
- [22] F. Martinez, G. Calleja, J.A. Melero, R. Molina, Heterogeneous photo-Fenton degradation of phenolic aqueous solutions over iron-containing SBA-15 catalyst, *Appl. Catal. B* 60 (3–4) (2005) 181–190.
- [23] C.S. Chiou, Y.H. Chen, C. Chang-Tang, C.Y. Chang, J.L. Shie, Y.S. Li, Photochemical mineralization of di-N-butyl phthalate with  $H_2O_2/Fe^{3+}$ , *J. Hazard. Mater.* 135 (1–3) (2006) 344–349.
- [24] M. Perez-Moya, M. Graells, L.J. del Valle, E. Centelles, H.D. Mansilla, Fenton and photo-Fenton degradation of 2-chlorophenol: multivariate analysis and toxicity monitoring, *Catal. Today* 124 (3–4) (2007) 163–171.
- [25] S. Malato, P. Fernandez-Ibanez, M.I. Maldonado, J. Blanco, W. Gernjak, Decontamination and disinfection of water by solar photocatalysis: recent overview and trends, *Catal. Today* 147 (1) (2009) 1–59.
- [26] J. De Laat, H. Gallard, S. Ancelin, B. Legube, Comparative study of the oxidation of atrazine and acetone by  $H_2O_2/UV$ ,  $Fe(III)/UV$ ,  $Fe(III)/H_2O_2/UV$  and  $Fe(II)$  or  $Fe(III)/H_2O_2$ , *Chemosphere* 39 (15) (1999) 2693–2706.
- [27] M. Panizza, I. Sires, G. Cerisola, Anodic oxidation of mecoprop herbicide at lead dioxide, *J. Appl. Electrochem.* 38 (7) (2008) 923–929.
- [28] F. Torrades, M. Perez, H.D. Mansilla, J. Peral, Experimental design of Fenton and photo-Fenton reactions for the treatment of cellulose bleaching effluents, *Chemosphere* 53 (10) (2003) 1211–1220.
- [29] F. Wu, N.S. Deng, Photochemistry of hydrolytic iron (III) species and photoinduced degradation of organic compounds. A minireview, *Chemosphere* 41 (8) (2000) 1137–1147.
- [30] F. Torrades, S. Saiz, A. Garcia-Hortal, J. Garcia-Montano, Degradation of wheat straw black liquor by Fenton and photo-Fenton processes, *Environ. Eng. Sci.* 25 (1) (2008) 92–98.
- [31] F.A. Al Momani, A.T. Shawaqfeh, M.S. Shawaqfeh, Solar wastewater treatment plant for aqueous solution of pesticide, *Sol. Energy* 81 (10) (2007) 1213–1218.
- [32] M.R.A. Silva, A.G. Trovo, R.F.P. Nogueira, Degradation of the herbicide tebuthiuron using solar photo-Fenton process and ferric citrate complex at circumneutral pH, *J. Photochem. Photobiol. A* 191 (2–3) (2007) 187–192.
- [33] M.J. Xu, Q.S. Wang, Y.L. Hao, Removal of organic carbon from wastepaper pulp effluent by lab-scale solar photo-Fenton process, *J. Hazard. Mater.* 148 (1–2) (2007) 103–109.
- [34] J.J. Pignatello, Y.F. Sun, Complete oxidation of metolachlor and methyl parathion in water by the photoassisted Fenton reaction, *Water Res.* 29 (8) (1995) 1837–1844.
- [35] M.Y. Ghaly, G. Hartel, R. Mayer, R. Haseneder, Photochemical oxidation of p-chlorophenol by  $UV/H_2O_2$  and photo-Fenton process. A comparative study, *Waste Manage.* 21 (1) (2001) 41–47.
- [36] P. Bautista, A.F. Mohedano, M.A. Gilarranz, J.A. Casas, J.J. Rodriguez, Application of Fenton oxidation to cosmetic wastewaters treatment, *J. Hazard. Mater.* 143 (1–2) (2007) 128–134.
- [37] M. Perez, F. Torrades, X. Domenech, J. Peral, Fenton and photo-Fenton oxidation of textile effluents, *Water Res.* 36 (11) (2002) 2703–2710.
- [38] M.I. Pariente, F. Martinez, J.A. Melero, J.A. Botas, T. Velegraki, N.P. Xekoukoulotakis, D. Mantzavinos, Heterogeneous photo-Fenton oxidation of benzoic acid in water: effect of operating conditions, reaction by-products and coupling with biological treatment, *Appl. Catal. B* 85 (1–2) (2008) 24–32.
- [39] P. Kajitvichyanukul, M.C. Lu, A. Jamroensan, Formaldehyde degradation in the presence of methanol by photo-Fenton process, *J. Environ. Manage.* 86 (3) (2008) 545–553.
- [40] J. Bachman, H.H. Patterson, Photodecomposition of the carbamate pesticide carbofuran: kinetics and the influence of dissolved organic matter, *Environ. Sci. Technol.* 33 (6) (1999) 874–881.
- [41] Q.Q. Wang, A.T. Lemley, Oxidative degradation and detoxification of aqueous carbofuran by membrane anodic Fenton treatment, *J. Hazard. Mater.* 98 (1–3) (2003) 241–255.
- [42] W.S. Kuo, Y.H. Chiang, L.S. Lai, Degradation of carbofuran in water by solar photocatalysis in presence of photosensitizers, *J. Environ. Sci. Health. B* 41 (6) (2006) 937–948.